

Structure of a DNA–Porphyrin Complex<sup>†</sup>Leigh Ann Lipscomb,<sup>‡</sup> Fang Xiao Zhou,<sup>§</sup> Steven R. Presnell, Rebecca J. Woo, Mary E. Peek,<sup>||</sup> R. Richard Plaskon, and Loren Dean Williams\*

School of Chemistry and Biochemistry, Georgia Institute of Technology, Atlanta, Georgia 30332-0400

Received October 13, 1995; Revised Manuscript Received December 28, 1995<sup>⊗</sup>

**ABSTRACT:** We report the 2.4 Å resolution X-ray structure of a complex in which a small molecule flips a base out of a DNA helical stack. The small molecule is a metalloporphyrin, CuTMPyP4 [copper(II) *meso*-tetra(*N*-methyl-4-pyridyl)porphyrin], and the DNA is a hexamer duplex, [d(CGATCG)]<sub>2</sub>. The porphyrin system, with the copper atom near the helical axis, is located within the helical stack. The porphyrin binds by normal intercalation between the C and G of 5' TCG 3' and by extruding the C of 5' CGA 3'. The DNA forms a distorted right-handed helix with only four normal cross-strand Watson–Crick base pairs. Two pyridyl rings are located in each groove of the DNA. The complex appears to be extensively stabilized by electrostatic interactions between positively charged nitrogen atoms of the pyridyl rings and negatively charged phosphate oxygen atoms of the DNA. Favorable electrostatic interactions appear to draw the porphyrin into the duplex interior, offsetting unfavorable steric clashes between the pyridyl rings and the DNA backbone. These pyridyl–backbone clashes extend the DNA along its axis and preclude formation of van der Waals stacking contacts in the interior of the complex. Stacking contacts are the primary contributor to stability of DNA. The unusual lack of van der Waals stacking contacts in the porphyrin complex destabilizes the DNA duplex and decreases the energetic cost of local melting. Thus extrusion of a base appears to be facilitated by pyridyl–DNA steric clashes.

Some DNA repair and modification proteins bind specifically to extrahelical bases. Cytosine flips out of the DNA helical stack and into the active sites of 5-methyltransferases *HhaI* (Klimasauskas et al., 1994) and *HaeIII* (Reinisch et al., 1995). Uracil flips out of the DNA stack and into the active site of uracil–DNA glycosylase (Mol et al., 1995; Savva et al., 1995). Here we report the first X-ray structure in which a small molecule extrudes a base from the DNA stack. The small molecule is a metalloporphyrin, CuTMPyP4 [copper(II) *meso*-tetra(*N*-methyl-4-pyridyl)porphyrin, Figure 1], and the DNA is a hexamer duplex, [d(CGATCG)]<sub>2</sub>. The porphyrin binds to DNA (Figures 2 and 3) by a novel mode of interaction we designate “hemiintercalation” to indicate intercalation with one strand of duplex DNA but not the other.

Intercalators bind with greater than normal affinity to DNA that contains extrahelical structural elements. Bulges (a bulge is an extra, unpaired residue on one strand) and Holliday junctions confer greater than normal stability to intercalation (Nelson & Tinoco, 1985; Williams & Goldberg, 1988; Lu et al., 1992). Extrahelical structural elements such as flipped out bases, bulges, and junctions probably sponsor some common features in DNA. Thus binding of an intercalator near a flipped out base is not altogether unexpected. Previous work was designed to evaluate

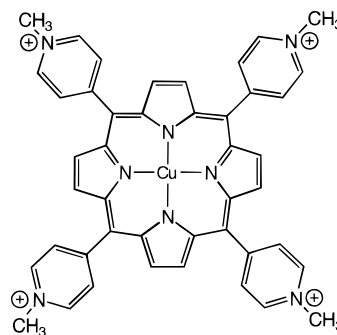


FIGURE 1: Chemical structure of CuTMPyP4 [copper(II) *meso*-tetra(*N*-methyl-4-pyridyl)porphyrin].

interactions with preexisting bulges and junctions. The present work is the first direct observation of an extrahelical structural element that has been induced by intercalation.

Extrahelical structural elements are thought to be intermediates in mutagenesis, and their stabilization by intercalators *in vivo* may be a factor in certain mutagenic pathways. If extrahelical structural elements are stabilized by small molecules acting at the DNA level, small molecules might alter energetic profiles of many DNA repair, modification, and recombination processes.

Porphyrins intercalate in DNA with binding constants of around 10<sup>6</sup> M<sup>-1</sup> (Fiel et al., 1979; Pasternack et al., 1986; Sari et al., 1990). Tetrapyrrolylporphyrins are much larger than conventional intercalators, and one might expect kinetic and thermodynamic barriers to their intercalation. Entry into DNA may require conformational distortion reaching the limit of DNA melting. Our results are consistent with severe conformational distortion left unresolved upon achievement of the ground-state complex. Steric clashing between the DNA backbone and the porphyrin pyridyl groups extends the DNA along its helical axis, destacking the interior of the complex.

<sup>†</sup> This work was supported by the American Cancer Society (NP-912), the National Science Foundation (MCB-9506300), the Pittsburgh Supercomputing Center (MCB950015P), and the NIH (Fellowship 5F32-CA65088 to L.A.L.).

\* Author to whom correspondence should be addressed.

<sup>‡</sup> Present address: Institute of Molecular Biology, University of Oregon, Eugene, OR 97403.

<sup>§</sup> Present address: Department of Molecular Biophysics and Biochemistry, Yale University, New Haven, CT 06520.

<sup>||</sup> Present address: Massey Cancer Center, Medical College of Virginia, Richmond, VA 23298.

<sup>⊗</sup> Abstract published in *Advance ACS Abstracts*, February 1, 1996.

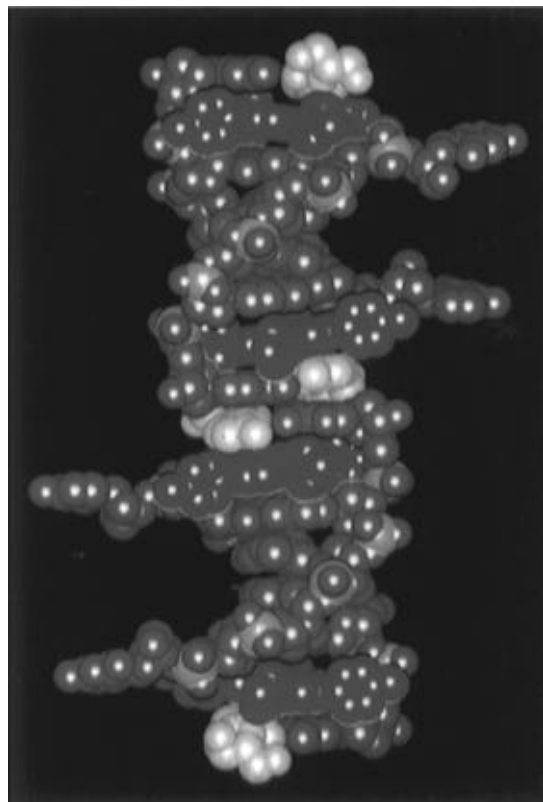


FIGURE 2: Space-filling representation of a continuous helix as observed in the  $d(\text{CGATCG})\cdot\text{CuTMPyP4}$  crystal. The DNA is in blue with phosphorus atoms in gold to highlight the phosphodiester backbone. Porphyrin molecules are in red. Cytidine residues from adjacent stacks in the crystal are in purple. The asymmetric unit contains one strand of DNA and one CuTMPyP4 molecule. The second strand of the DNA duplex and the second CuTMPyP4 molecule are generated with the symmetry operator  $x, x - y - 1, 7/6 - z$ . The second duplex stacked along the crystallographic  $c$ -axis (vertical) is generated with  $-x, -x + y, -z + 2/3$ . Purple cytosines are generated with (1)  $-y, x - y - 1, z + 1/3$ , (2)  $-y, -x, 5/6 - z$ , (3)  $y, y - x, 5/6 + z - 1$ , and (4)  $y, x - 1, 1/3 - z$ . This representation was generated with INSIGHTII (1991).

## MATERIALS AND METHODS

**Crystallization.** The ammonium salts of reverse-phase, HPLC-purified  $d(\text{CGATCG})$  and  $d(\text{CGAT}^1\text{CG})$  (where  $^1\text{C} = 5\text{-iodocytidine}$ ) were obtained from Midland Certified Reagent Co. (Midland, TX). CuTMPyP4 chloride (Midcentury Chemicals, Posen, IL) was used without purification. Crystals were grown in sitting drops by vapor diffusion. Crystals of  $d(\text{CGATCG})\cdot\text{CuTMPyP4}$  were grown from a solution initially containing 0.9 mM DNA (single-strand concentration), 1.0 mM CuTMPyP4, 1.0% 2-methyl-2,4-pentanediol (MPD), 2.1 mM magnesium chloride, 2.1 mM spermine hydrochloride, and 40.0 mM sodium cacodylate (pH 6.5). Drops were equilibrated against a reservoir of 30% MPD. Deep red crystals appeared within 9 days and within 8 weeks grew to a size of  $0.60 \times 0.35 \times 0.35$  mm. Crystals of  $d(\text{CGAT}^1\text{CG})\cdot\text{CuTMPyP4}$  were grown from solution initially containing 0.5 mM  $d(\text{CGAT}^1\text{CG})$ , 0.5 mM CuTMPyP4, 0.5% MPD, 1.0 mM magnesium chloride, 0.5 mM spermine hydrochloride, and 40.0 mM sodium cacodylate (pH 6.5). These drops were equilibrated against a reservoir of 20% MPD. Crystals appeared within 9 days and within 8 weeks grew to a size of  $0.41 \times 0.20$  mm.

**Soaking.**  $\text{K}_2\text{PtCl}_4$  was added to sitting drops containing crystals of  $d(\text{CGATCG})\cdot\text{CuTMPyP4}$  such that the final

concentration of  $\text{K}_2\text{PtCl}_4$  was 2.5 mM. Crystals were soaked for 1 week at 23 °C [then referred to as  $d(\text{CGATCG}^{\text{Pt}})\cdot\text{CuTMPyP4}$ ] prior to mounting, unit cell determination, and data collection. The  $d(\text{CGATCG}^{\text{Pt}})\cdot\text{CuTMPyP4}$  crystal used for data collection was  $0.44 \times 0.18 \times 0.18$  mm.

**X-ray Diffraction.** A crystal was sealed in a glass capillary with a droplet of mother liquor and mounted on a Huber goniostat. Copper  $\text{K}\alpha$  radiation ( $\lambda = 1.5418 \text{ \AA}$ ) was generated with a fine-focus Rigaku RU-200 rotating anode. Unit cell parameters for crystals of  $d(\text{CGATCG})\cdot\text{CuTMPyP4}$  were  $a = b = 39.49 \text{ \AA}$ ,  $c = 56.15 \text{ \AA}$ ,  $\alpha = \beta = 90.0^\circ$ ,  $\gamma = 120.0^\circ$ . The crystallographic space group, determined by precession photography, is  $P6_1(5)22$ .  $P6_122$  was selected as the correct space group because the other enantiomorph gave DNA with a left-handed helical twist.

X-ray intensity data were collected at 23 °C in the  $\omega$  scan mode with a San Diego Multiwire Systems area detector. Initial data were collected at full generator power (100 mA, 46 kV). The frames containing extremely intense "stacking" reflections were excluded from the data reduction process. To accurately measure intensities of the strong reflections, these frames were recollected at reduced power (50 mA, 46 kV) and scaled to the others. A total of 49 552 observations of 1334 unique reflections gave an  $R$ -merge [ $\sum |I_{\text{av}} - I|^2 / \sum |I_{\text{av}}|^2$ ] of 9.0% including all data to 2.3 Å resolution. Data reduction and MIR statistics are given in Table 1.

**Structure Solution.** Initially, molecular replacement seemed a reasonable approach to phase solution. The volume of a base pair is 1300–1600 Å<sup>3</sup>, and the volume of CuTMPyP4 is roughly equivalent to that of a base pair. Therefore, it was inferred that the most likely asymmetric unit ( $V = 6320 \text{ \AA}^3$ ) consists of one strand of DNA hexamer and one porphyrin molecule. If one strand is contained in the asymmetric unit and the DNA forms a duplex, that duplex must contain at its center one of the two crystallographic 2-fold axes. Native Patterson maps ( $F_o^2$ ) indicated 16 molecular planes (DNA base pairs or porphyrin molecules) stacked with normals roughly along the direct crystallographic  $c$ -axis. A continuous stack along the  $c$ -axis is generated by locating a second crystallographic 2-fold axis between duplexes, each containing two intercalated porphyrin molecules. The distance between the 2-fold axes is consistent with this model. Remaining unknowns are strand direction, intraduplex 2-fold and interduplex 2-fold. However, even with so few unknowns, molecular replacement failed because the starting model was inaccurate.

The  $d(\text{CGATCG})\cdot\text{CuTMPyP4}$  structure was solved by multiple isomorphous replacement (MIR) techniques using data from isomorphous iodine [ $d(\text{CGAT}^1\text{CG})\cdot\text{CuTMPyP4}$ ] and platinum [ $d(\text{CGATCG}^{\text{Pt}})\cdot\text{CuTMPyP4}$ ] derivatives. PHASES (Furey & Swaminathan, 1990) was used for refinement of heavy atom parameters, phase calculations, solvent flattening, phase recombination, and some map calculations. The X-PLOR package (Version 3.4) (Brunger, 1992) was used for refinement, simulated annealing, calculation of Wilson plots, and some map calculations. Difference Pattersons were solved by hand and with the program HASSP (Terwilliger et al., 1987). Display of maps and models and manipulation of models were performed with the program CHAIN (Sack, 1990) on a SGI Indigo2.

Wilson plots indicated that isotropic scaling of heavy to native structure factor amplitudes would be insufficient. Amplitudes were scaled first anisotropically with the program

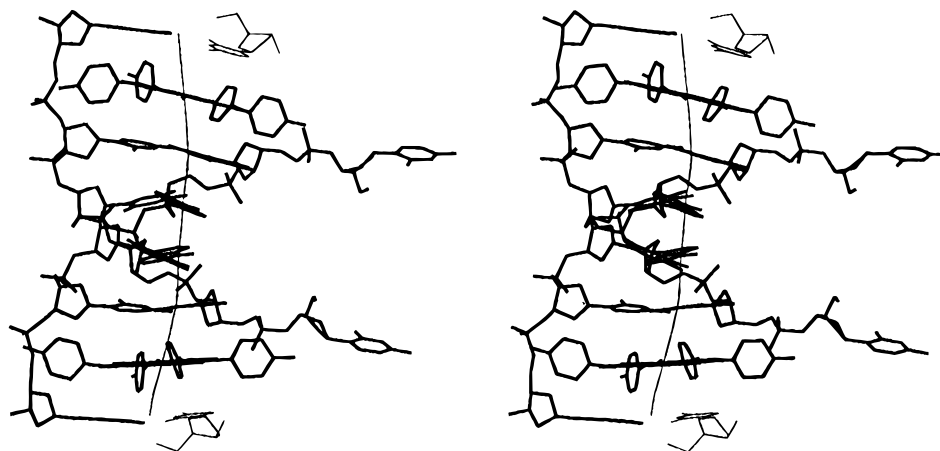


FIGURE 3: Stereoview stick representation of the d(CGATCG)·CuTMPyP4 complex. The DNA duplex and both porphyrin molecules are drawn with thick lines. Cytidine residues from adjacent stacks in the crystal are drawn in thin lines. The helical axis is indicated.

Table 1: Structure Solution and Refinement

	Heavy Atom Statistics		d(CGATCG) <sup>Pl</sup> ·CuTMPyP4
	d(CGATCG)·CuTMPyP4 data set 1	d(CGATCG) <sup>Pl</sup> ·CuTMPyP4 data set 2	
resolution (Å)	2.7	3.3	3.3
R-merge (%)	9.8	9.4	8.4
refined heavy atom position (x, y, z)	0.36064, 0.01838, 0.15805	0.36602, 0.02579, 0.15694	0.05060, 0.38905, 0.30944
B-factor (Å <sup>2</sup> )	52.20	19.12	34.04
cross R-factor (%)	28.7	28.4	36.2
occupancy	1.0	1.0	0.25
phasing power to 3.5 Å resolution	1.70	1.51	1.34

Figure of Merit (FOM) by Resolution Range<sup>a</sup>

mean resolution (Å)	mean FOM	mean resolution (Å)	mean FOM
10.03	0.672	4.45	0.519
7.20	0.728	4.16	0.602
6.09	0.554	3.93	0.585
5.35	0.628	3.73	0.405
4.86	0.698	3.51	0.503

Refinement Statistics

resolution range (Å)	no. of reflections	R-factor (%) <sup>b</sup>	completeness (%)
4.53–8.00	150	19.1	94.3
3.71–4.53	145	21.4	95.2
3.28–3.71	124	21.8	93.7
3.00–3.28	128	20.1	91.9
2.79–3.00	108	27.5	89.4
2.63–3.00	93	25.3	86.7
2.51–2.63	102	25.8	84.3
2.40–2.51	87	25.5	81.5

rms deviation of bonds from ideality = 0.015 Å

rms deviation of angles from ideality = 3.16°

<sup>a</sup> The overall FOM was 0.588 Å to 3.5 Å resolution, for 319 phased reflections. <sup>b</sup> The final R-factor is 21.9% to 2.4 Å resolution [1.5σ(F<sub>o</sub>)].

XtalView (McRee, 1992) and then locally with the program MAXSCALE (M. Rould, MIT). The iodine atom of d(CGATCG)·CuTMPyP4 was located by difference Patterson [(F<sub>n,o</sub> - F<sub>i,o</sub>)<sup>2</sup>, where F<sub>n,o</sub> and F<sub>i,o</sub> are observed native and iodine derivative structure factor amplitudes, respectively]. The position and B-factor were refined against centric (F<sub>n,o</sub> - F<sub>i,o</sub>)<sup>2</sup> using data to 3.0 Å resolution. The position of the iodine atom was used to calculate single isomorphous replacement (SIR) phases (α), improved by solvent flattening (Wang, 1985) (estimated solvent content = 30%). A cross-difference Fourier map [(F<sub>n,o</sub> - F<sub>pt,o</sub>)e<sup>-iα</sup>], where F<sub>pt,o</sub> is the platinum derivative structure factor amplitude] revealed a single platinum peak. The position

of the platinum atom was verified by difference Patterson [(F<sub>n,o</sub> - F<sub>pt,o</sub>)<sup>2</sup>]. Platinum position and B-factor were refined as described above for iodine. Also in analogy with the description above, the position of the iodine atom was confirmed by solvent-flattened platinum SIR phases.

MIR phases (α'), improved by solvent flattening, were estimated from the native, iodine, and platinum structure factor amplitudes. A cross-difference Fourier map [(F<sub>n,o</sub> - F<sub>pt,o</sub>)e<sup>-iα'</sup>] did not show additional platinum peaks. An MIR map (F<sub>n,o</sub>e<sup>-iα'</sup>) revealed the DNA backbone and a rough outline of the porphyrin (Figure 4). A partial model [residues A(3), T(4), and C(5)] was built into the MIR map. Each residue was refined as a rigid body against F<sub>n,o</sub> to 3.5 Å resolution. The refined coordinates were used for phase combination with the original MIR phases and to calculate sum (2F<sub>n,o</sub> - F<sub>n,c</sub>, where c indicates calculated) and difference (F<sub>n,o</sub> - F<sub>n,c</sub>) maps. These maps showed the position of residue C(1), which was added to the model. Cycles of rigid body refinement, phase recombination, and sum and difference map calculation were repeated until all atoms were located.

**Refinement.** Ideal geometry of CuTMPyP4 was based on the crystal structure of H<sub>2</sub>TMPyP4 (Ford et al., 1987), and geometry was sustained by approximate force constants (QUANTA, 1992). Bond lengths and angles, and planarities of the porphyrin ring and pyridyl groups, but not rotations about porphyrin-pyridyl bonds, were restrained. Charges for CuTMPyP4 were estimated from charges of ZnTMPyP4 obtained from one self-consistent field calculation with MOPAC 6.0 (Stewart, 1991) using the MNDO Hamiltonian. For the DNA, polar hydrogen atoms but not nonpolar hydrogen atoms were treated explicitly (Brooks et al., 1983).

Atomic positions were initially refined using all data to 2.7 Å resolution (R-factor of 39.8%). Simulated annealing (starting temperature 3000 K) decreased the R-factor to 37.1%. Refined omit maps were prepared for each DNA residue, the copper atom, the porphyrin ring, and the porphyrin pyridyl groups. These maps allowed for a correction of an error in topology and in position of the phosphate group of G(6). Refinement of the improved model decreased the R-factor to 34.5% to 2.7 Å resolution. Refinement of B-factors and anisotropic scaling of F<sub>n,o</sub> to F<sub>n,c</sub> with the Xmerge subroutine of XtalView decreased the R-factor to 30.4% to 2.4 Å resolution. Twenty-nine solvent molecules were located in groups of ten or less from sum

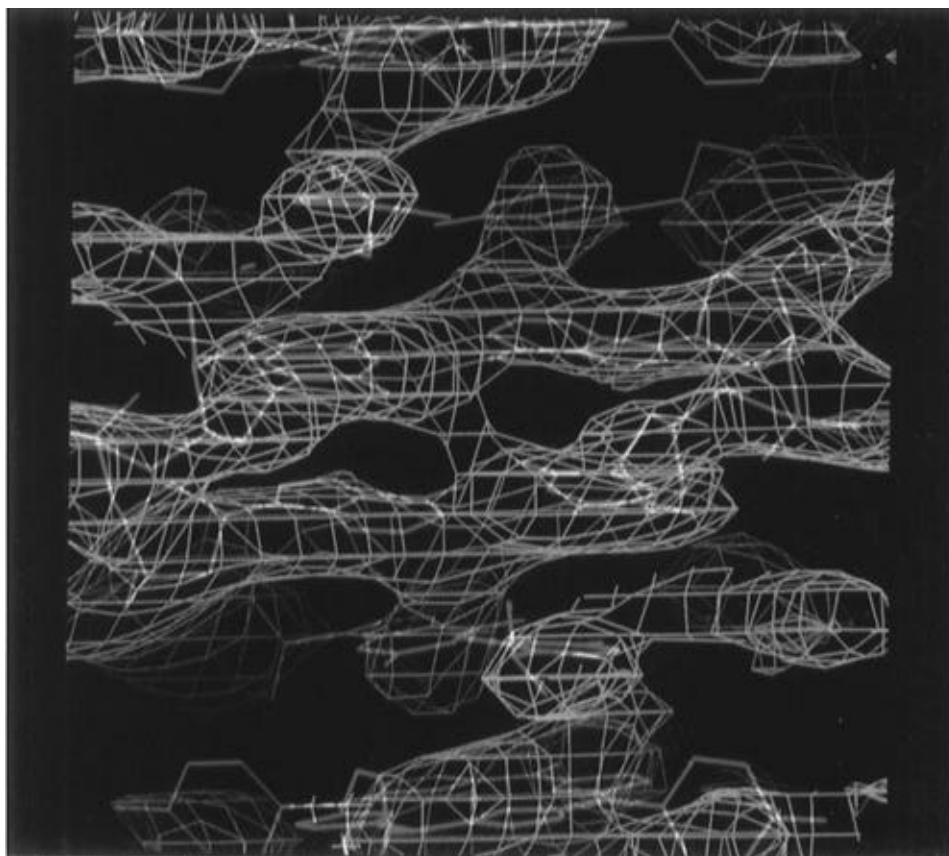


FIGURE 4: Solvent-flattened MIR map at 3.5 Å resolution. The final refined coordinates of d(CGATCG)·CuTMPyP4 are superimposed on the map.

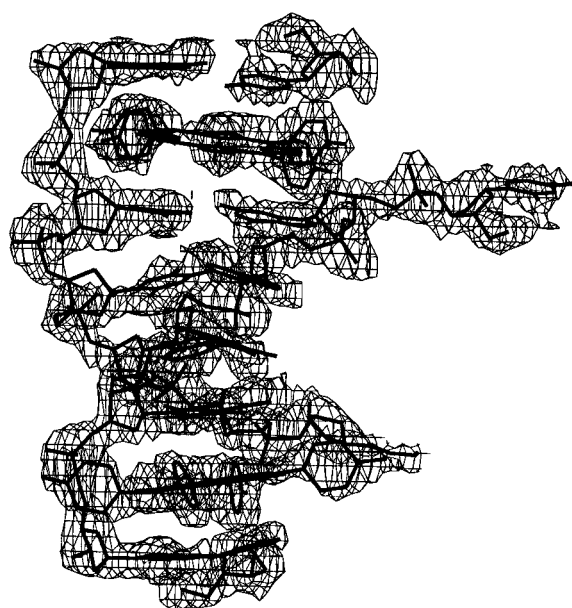


FIGURE 5: Sum electron density surrounding the d(CGATCG)·CuTMPyP4 complex.

( $2F_o - F_c$ ) and difference maps ( $F_o - F_c$ ). Positions and thermal factors of all atoms were refined after addition of solvent molecules. The refinement converged with an *R*-factor of 21.9% to 2.4 Å resolution (Table 1). Final Fourier sum density for the duplex is shown in Figure 5.

## RESULTS

The structure of the d(CGATCG)·CuTMPyP4 complex revealed unexpected features. The DNA forms a distorted

right-handed helix with only four normal cross-strand Watson–Crick base pairs. In comparison with B-DNA or other intercalated complexes, the porphyrin complex is extended along its axis, with an average helical rise of 3.6 Å. The center of the complex is bent toward the major groove. The DNA is unwound by a total of 35°, with unwinding confined predominantly to the intercalation step. The central AT base pairs display a large negative propeller twist of  $-29.8^\circ$ . This propeller twist brings the O4 of T(4) to within 3.21 Å of the N4 of C(5). However, consideration of the hydrogen bond geometry suggests that the O4 atom of T(4) does not form a hydrogen bond with the N4 atom of C(5). The glycosidic bond torsion angle ( $\chi = 3.0^\circ$ ) indicates the flipped out cytosine is in the syn conformation. In general, the backbone torsion angles are dissimilar to those of complexes of other intercalators of similar DNA sequence [d(CGATCG)·adriamycin (Frederick et al., 1990) or d(<sup>m5</sup>CGTsA<sup>m5</sup>CG)·nogalamycin (Williams et al., 1990a)] or of different DNA sequence [d(CGCG)<sub>2</sub>·ditercalinium (Williams & Gao, 1992)].

The porphyrin hemiintercalates at each C-G step of [d(CGATCG)<sub>2</sub>] such that two porphyrin molecules bind to each hexamer duplex (Figures 2 and 3). The term hemiintercalation is intended to specify intercalation within one strand of DNA but not the other. The porphyrin binds by normal intercalation between the C and G of 5' TCG 3' and by extruding the C of '5 CGA 3'. Cytosine (1) is flipped out of the helical stack. This base is involved in favorable lattice interactions. It is inserted into an adjacent stack in the crystal where it forms Watson–Crick hydrogen bonds with a guanine. The normal pairing partner of that guanine has been flipped out of its stack. In this manner, every base in the complex is located within a helical stack forming Watson–Crick hydrogen bonds. However, only four of the

six base pairs of each hexamer duplex are between bases of opposing strands.

The porphyrin does not form van der Waals stacking contacts with adjacent bases even though the porphyrin heterocycle is located directly within the DNA helical stack and the copper atom is near the helical axis. Of the 10 DNA–porphyrin van der Waals contacts (criterion is interatomic distance  $<3.35 \text{ \AA}$ ) in the complex, nine are between pyridyl groups and the DNA backbone while only one is between the porphyrin heterocycle and a DNA base. By contrast, one intercalated chromophore in the  $d(\text{CGCG})_2$  ditercalinium structure (Williams & Gao, 1992) has 28 van der Waals contacts with DNA bases. We infer that the porphyrin–backbone contacts are steric clashes that extend the helix along its axis and prevent formation of stable van der Waals stacking contacts between bases and the porphyrin heterocycle. In normal DNA, extrusion of a base requires disruption of favorable van der Waals stacking contacts. However, stacking contacts are virtually absent from the interior of the porphyrin complex. Thus the relative stability of the extruded conformation is increased upon binding of the porphyrin.

The porphyrin complex appears to be stabilized by extensive electrostatic interactions, especially in the minor groove. In the complex, two positively charged pyridyl groups are located in the minor groove and are in close proximity to several negatively charged phosphate oxygen atoms. The pyridyl nitrogen of each minor groove ring is nearby four phosphate oxygen atoms (3.95, 5.55, 7.88, and 9.41  $\text{\AA}$  for one pyridyl nitrogen and 4.90, 4.94, 6.45, and 6.24  $\text{\AA}$  for the other). Two pyridyl groups are located in the major groove of the complex and but are relatively far away from phosphate oxygen atoms (8.94, 6.64, and 8.74  $\text{\AA}$  for one pyridyl nitrogen, no phosphate oxygen atoms less than 10.0  $\text{\AA}$  from the other). In the minor groove, a solvent molecule, possibly a sodium ion, is located on the crystallographic 2-fold axis with close contacts (2.48  $\text{\AA}$ ) with T(4) O2 and T(10) O2.

## DISCUSSION

We report the structure of a DNA–porphyrin complex. Porphyrin molecules hemiintercalate at the C-G steps of  $[d(\text{CGATCG})]_2$  such that two porphyrins bind to each hexamer duplex. The porphyrin binds by normal intercalation between the C and G of 5' TCG 3' and by extruding the C of 5' CGA 3'. The DNA forms a distorted right-handed helix with only four cross-strand Watson–Crick base pairs. The porphyrin system is located within the helical stack, with the copper atom near the helical axis. Two pyridyl rings are located in each groove of the DNA. The complex appears to be extensively stabilized by electrostatic interactions between positively charged nitrogen atoms of the pyridyl rings and negatively charged phosphate groups of the DNA. A schematic diagram of a porphyrin hemiintercalated in a long fragment of DNA is shown in Figure 6.

Strong electrostatic forces appear to draw the porphyrin into the duplex interior, offsetting unfavorable steric clashes between the pyridyl rings and the DNA backbone. The pyridyl–backbone clashes extend the DNA along its axis and preclude van der Waals stacking contacts in the interior of the complex. Stacking contacts are the primary contributor to stability of DNA. We propose that a lack of van der Waals stacking contacts with the porphyrin destabilizes the

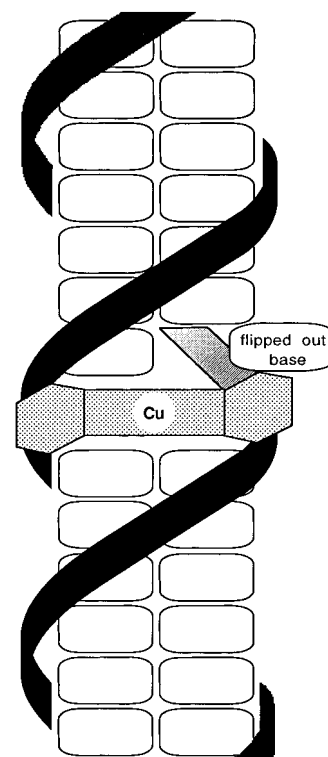


FIGURE 6: Schematic diagram of a porphyrin hemiintercalated in a fragment of DNA.

flanking base pairs, decreasing the energetic cost of local melting. Thus extrusion of a base appears to be facilitated by pyridyl–DNA steric clashes.

A retrospective analysis finds solution evidence for hemiintercalation of porphyrins and extrusion of bases from helical stacks. Marzilli et al. (1986) showed with solution  $^1\text{H}$  and  $^{31}\text{P}$  NMR that porphyrins bind at the central 5'–CpG–3' step of  $[d(\text{TATATGCGCATATA})]_2$ . The imino resonances of the guanines on either side of the binding site are unobservable, most probably because of rapid exchange with aqueous solvent. This result is consistent with disruption of base pairs, or decreased base pair lifetime, as expected in a static or transient hemiintercalated complex. In addition, the observation that porphyrins “pseudointercalate” in single-stranded DNA (Carvlin & Fiel, 1983; Pasternack et al., 1990) provides precedence for hemiintercalation, in which a porphyrin intercalates in one strand of duplex DNA. Additional support for hemiintercalation in solution is the preferential binding of porphyrins to melted or partially melted regions of DNA (Raner et al., 1988).

Fiel et al. (1979) were the first to suggest, from unwinding and lengthening of DNA, that porphyrins intercalate in DNA. Porphyrins also bind via outside, nonintercalative modes (Carvlin & Fiel, 1983). Mode of binding is controlled by porphyrin shape and charge. Ligands at the fifth and sixth coordination sites of the metal sterically block intercalation. Thus metal-free  $\text{H}_2\text{TMPyP}_4$  and four-coordinate porphyrins ( $\text{NiTMPyP}_4$ ,  $\text{CuTMPyP}_4$ , and  $\text{PdTMPyP}_4$ ) intercalate, while five- and six-coordinate porphyrins ( $\text{MnTMPyP}_4$ ,  $\text{FeTMPyP}_4$ ,  $\text{CoTMPyP}_4$ , and  $\text{ZnTMPyP}_4$ ) bind via nonintercalative modes (Banville et al., 1983; Pasternack et al., 1983). Porphyrins are therapeutically useful, playing a role in photodynamic therapy (Pass, 1993). Upon irradiation, certain porphyrins and porphyrin-like molecules cleave and cross-link DNA and cause sister chromatid exchange (Kvam & Stokke, 1994).

To help determine which structural features of the porphyrin drive the complex away from normal intercalation toward hemiintercalation, we constructed a molecular model in which CuTMPyP4 is normally intercalated at both 5'-CpG-3' steps of d(CGATCG). The model was prepared by flipping each extrahelical cytosine of the X-ray structure back into the duplex to form hydrogen bonds with its Watson-Crick cross-strand partner. The energy of the model was minimized with X-PLOR. Atomic positions for CuTMPyP4 and residues A(3), T(4), C(5), and G(6) were held fixed during energy minimization of packing van der Waals, packing electronic, bonding, angle, dihedral, improper, van der Waals, electronic, and planarity terms. After minimization, the energy of the normally intercalated model is 8.5% higher than that of the original hemiintercalated structure. The normally intercalated model, like the original structure, is characterized by extensive electrostatic interactions but poor van der Waals stacking interactions. In summary, normal intercalation of CuTMPyP4 and other such large intercalators appears to be stereochemically feasible but is destabilized by disruption of van der Waals stacking contacts.

The structure described here does not directly address the issue of whether hemiintercalated complexes predominate in solution or represent minor components that have selectively crystallized in this case. However, previous evidence for hemiintercalation of porphyrins and extrusion of bases from the helical stack in solution (above) suggests hemiintercalated structures are a significant fraction of the solution population. This scenario is consistent with the observation that DNA complexes with intercalators show considerably fewer lattice effects than uncomplexed DNA (Williams et al., 1990b). Effects of lattice are conspicuously absent from X-ray structures of intercalated DNA, in part because conventional intercalation stiffens DNA, causing DNA-intercalator complexes to be less polymorphic in solution than DNA alone.

The d(CGATCG)·CuTMPyP4 structure described here could help explain aspects of electron-transfer processes in DNA. It was suggested that DNA provides an effective medium for long-range electron transfer (Murphy et al., 1993). Specifically, DNA may convey electrons between metal-containing intercalators over relatively great distances. However, many issues surrounding electron transfer in DNA remain unresolved. Brun and Harriman (1994) conclude that DNA is a poor medium for electron exchange between palladium porphyrins bound to DNA. The structure described here is the first in which a metal atom resides near the central normal of a base pair plane, near the DNA helical axis. A potential for poor van der Waals stacking contacts should be considered in evaluating electron transfer between an intercalated (or hemiintercalated) porphyrin system and adjacent DNA bases.

#### ACKNOWLEDGMENT

The authors thank B.-C. Wang, M. Rould, H. Drew, T. Terwilliger, W. Furey, J. Haseltine, R. F. Pasternack, and L. Marzilli for helpful discussions. Coordinates were deposited in the Brookhaven Protein Data Bank (ID code 231D).

#### REFERENCES

Banville, D. L., Marzilli, L. G., & Wilson, W. D. (1983) *Biochem. Biophys. Res. Commun.* 113, 148–154.

- Brooks, B. R., Brucoli, R. E., Olafson, B. D., States, D. J., Swaminathan, S., & Karplus, M. (1983) *J. Comput. Chem.* 4, 187–217.
- Brun, A. M., & Harriman, A. (1994) *J. Am. Chem. Soc.* 116, 10383–10393.
- Brunger, A. (1992) *X-PLOR Software*, The Howard Hughes Medical Institute and Yale University, New Haven, CT.
- Carvlin, M. J., & Fiel, R. J. (1983) *Nucleic Acids Res.* 11, 6121–6139.
- Fiel, R. J., Howard, J. C., Mark, E. H., & Datta Gupta, N. (1979) *Nucleic Acids Res.* 6, 3093–3118.
- Ford, K. G., Pearl, L. H., & Neidle, S. (1987) *Nucleic Acids Res.* 15, 6553–6562.
- Frederick, C. A., Williams, L. D., Ughetto, G., van der Marel, G. A., van Boom, J. H., Rich, A., & Wang, A. H.-J. (1990) *Biochemistry* 29, 2538–2549.
- Furey, W., & Swaminathan, S. (1990) *Proc. Am. Cryst. Assoc. Natl. Meet.*, PA33, 73.
- INSIGHTII (1991) BIOSYM Technologies, San Diego, CA.
- Klimasauskas, S., Kumar, S., Roberts, R. J., & Cheng, X. (1994) *Cell* 76, 357–369.
- Kvam, E., & Stokke, T. (1994) *Photochem. Photobiol.* 59, 437–40.
- Lu, M., Guo, Q., & Kallenbach, N. R. (1992) *Crit. Rev. Biochem. Mol. Biol.* 27, 157–190.
- Marzilli, L. G., Banville, D. L., Zon, G., & Wilson, W. D. (1986) *J. Am. Chem. Soc.* 108, 4188–4192.
- McRee, D. E. (1992) *J. Mol. Graphics* 10, 44–46.
- Mol, C. D., Arvai, A. S., Slupphaug, G., Kavli, B., Alseth, I., Krokan, H. E., & Tainer, J. A. (1995) *Cell* 80, 869–878.
- Murphy, C. J., Arkin, M. R., Jenkins, Y., Ghatlia, N. D., Bossmann, S. H., Turro, N. J., & Barton, J. K. (1993) *Science* 262, 1025–1029.
- Nelson, J. W., & Tinoco, I., Jr. (1985) *Biochemistry* 24, 6416–6421.
- Pass, H. I. (1993) *J. Natl. Cancer Inst.* 85, 443–456.
- Pasternack, R. F., Gibbs, E. J., & Villafranca, J. J. (1983) *Biochemistry* 22, 2406–2414.
- Pasternack, R. F., Garrity, P., Ehrlich, B., Davis, C. B., Gibbs, E. J., Orloff, G., Giartosio, A., & Turano, C. (1986) *Nucleic Acids Res.* 14.
- Pasternack, R. F., Brigandi, R. A., Abrams, M. J., Williams, A. P., & Gibbs, E. J. (1990) *Inorg. Chem.* 29, 4483–4486.
- QUANTA (1992) *Parameter Handbook, Version 3.3*, Molecular Simulations, Waltham, MA.
- Raner, G. R., Ward, B., & Dabrowiak, J. C. (1988) *J. Coord. Chem.* 19, 17–23.
- Reinisch, K., Chen, L., Verdine, G. L., & Lipscomb, W. N. (1995) *Cell* 82, 143–153.
- Sack, J. (1990) *Chain: A Crystallographic Modelling Program*, Baylor College of Medicine, Waco, TX.
- Sari, M. A., Battioni, J. P., Dupre, D., Mansuy, D., & Le Pecq, J. B. (1990) *Biochemistry* 29, 4205–4215.
- Savva, R., McAuley-Hecht, K., Brown, T., & Pearl, L. (1995) *Nature (London)* 373, 487–493.
- Stewart, J. J. P. (1991) *QCPE Catalogue*, Vol. XXIII, Program number 455.
- Terwilliger, T. C., Kim, S.-H., & Eisenberg, D. (1987) *Acta Crystallogr.* A43, 1–5.
- Wang, B.-C. (1985) in *Methods in Enzymology* (Colowick, S. P., & Kaplan, N. O., Eds.) Vol. 115, pp 90–112, Academic Press, Orlando, FL.
- Williams, L. D., & Gao, Q. (1992) *Biochemistry* 31, 4315–4324.
- Williams, L. D., & Goldberg, I. H. (1988) *Biochemistry* 27, 3004–3011.
- Williams, L. D., Egli, M., Gao, Q., Bash, P., van der Marel, G. A., van Boom, J. H., Rich, A., & Frederick, C. A. (1990a) *Proc. Natl. Acad. Sci. U.S.A.* 87, 2225–2229.
- Williams, L. D., Egli, M., Ughetto, G., van der Marel, G. A., van Boom, J. H., Quigley, G. J., Wang, A. H.-J., Rich, A., & Frederick, C. A. (1990b) *J. Mol. Biol.* 215, 313–320.